Article

Hydrostatic Pressure Effect on the Phase Transitions of a Closed-Loop Type Block Copolymer by Using 2D FTIR Correlation Spectroscopy

Hye Jeong Kim, Seung Bin Kim, Jin Kon Kim, and Young Mee Jung

J. Phys. Chem. B, **2008**, 112 (48), 15295-15300• DOI: 10.1021/jp806019n • Publication Date (Web): 31 October 2008

Hydrostatic Pressure Effect on the Phase Transitions of a Closed-Loop Type Block Copolymer by Using 2D FTIR Correlation Spectroscopy

Hye Jeong Kim,[†] Seung Bin Kim,*[,‡] Jin Kon Kim,*[,†] and Young Mee Jung[§]

National Creative Research Center for Block Copolymer Self-Assembly, Department of Chemical Engineering, Department of Chemistry, Pohang University of Science and Technology, Kyungbuk 790-784, Korea, and Department of Chemistry, Kangwon National University, Chunchon 200-701, Korea

Received: July 8, 2008; Revised Manuscript Received: August 26, 2008

The effect of hydrostatic pressure (*P*) on the phase transitions of polystyrene-*block*-poly(*n*-pentyl methacrylate) copolymer [PS-b-PnPMA] was investigated with FTIR spectroscopy at various temperatures. The experiments were performed by using a specially designed pressure cell optimized for low-pressure regime (<100 bar) with a higher resolution (~1 bar). The size of the closed loop consisting of both the lower disorder-to-order transition (LDOT) and the upper order-to-disorder transition (UODT) measured by FTIR spectroscopy becomes smaller with increasing *P*, consistent with results obtained from birefringence measurement. At lower temperatures with increasing *P*, the PS main chains are found to move before the PnPMA main chains. This is because the mobility of the PnPMA main chains is restricted due to the cluster formation of the alkyl side chain. At higher temperatures, the PnPMA block chains are more mobile than the PS block chains due to their larger specific volumes. The results indicate that the LDOT is mainly affected by a favorable directional interaction between PS and PnPMA blocks due to the cluster formation of the alkyl side chain, whereas the UODT depends on the combinatorial entropy.

1. Introduction

The phase behavior of block copolymers has been extensively studied due to the self-assembly with nanometer sizes.[1−30] Block copolymers generally exhibit an ordering transition upon cooling, which is referred to as the order-to-disorder transition (ODT) or the upper order-to-disorder transition (UODT),[5−10] whereas some block copolymers are known to undergo an ordering transition upon heating, which is referred to as a lower disorder-to-order transition (LDOT).[11−17] Unlike ODT, the hydrostatic pressure (*P*) dramatically changed LDOT.[13,14]

We reported that polystyrene-*block*-poly(*n*-pentyl methacrylate) copolymers (PS-PnPMA) were shown to exhibit a closed loop type of phase behavior, where upon heating an LDOT was found at lower temperature and a UODT was observed at higher temperature.[18−26] We also showed that *P* significantly affected the transition temperature of deuterated polystyrene-*block*-poly(n-pentyl methacrylate) (dPS-PnPMA) by using small-angle neutron scattering (SANS) and birefringence.[20] Cho and coworkers[27] suggested that a specific interaction as well as free volume effect should be introduced to explain the closed loop phase behavior. However, the details of the specific interaction, especially the pressure effect on this interaction, of PS-PnPMA remain to be solved. This kind of the information needs molecular level study of both of the block chains.

We recently determined the transition temperatures of PS-PnPMA at ambient pressure by FTIR spectroscopy.[28−30] The measurements showed that a favorable directional interaction between the PS and PnPMA blocks is due to the dipole in the PS phenyl ring and an induced dipole of PnPMA resulting from the formation of 1−2 nm clusters.[29] These results imply that the disordered state at lower temperatures is due primarily to the favorable interaction, whereas the disordered state at higher temperatures arises from an increase in the combinatorial entropy, though a tiny favorable interaction might exist.[28−30]

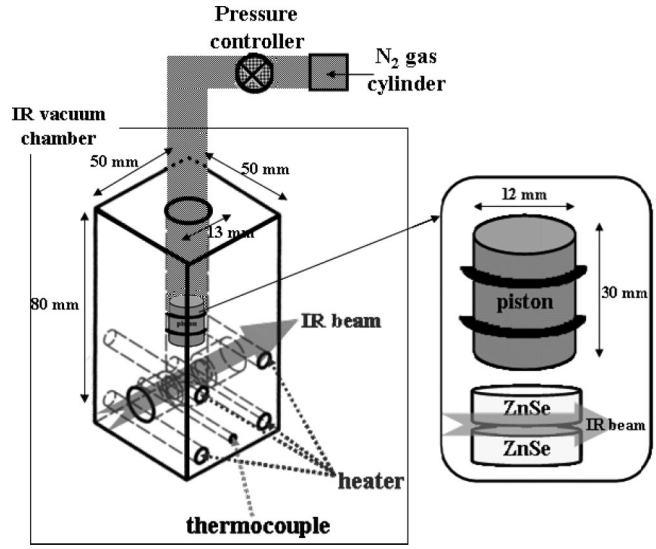

Figure 1. Pressure cell employed for FTIR experiment.

It is important to understand the detailed mechanisms related to the pressure dependence on the phase transitions, since the phase transitions of PS-PnPMA are significantly affected by *P*.[20] The transition temperatures and their pressure dependence are easily determined by using small-angle neutron scattering and birefringence methods; however, these methods cannot provide information on the transition mechanisms at the molecular level of the block chains.

* To whom correspondence should be addressed. E-mail: (J.K.K.) jkkim@postech.ac.kr; (S.B.K.) sbkim@postech.ac.kr.

[†] National Creative Research Center for Block Copolymer Self-Assembly, Department of Chemical Engineering, Pohang University of Science and Technology.

[‡] Department of Chemistry, Pohang University of Science and Technology.

[§] Kangwon National University.

10.1021/jp806019n CCC: $40.75
Published on Web 11/01/2008

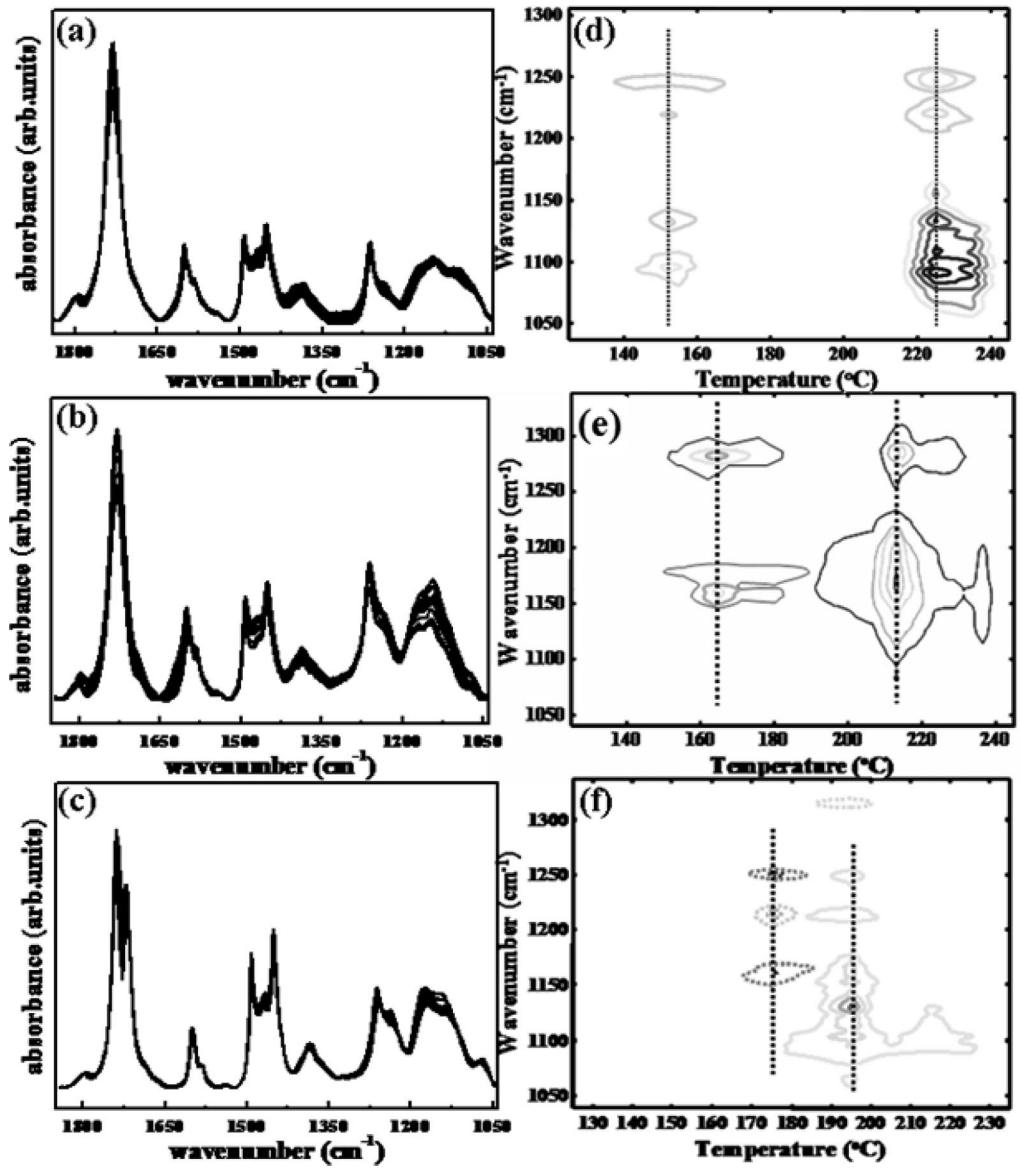

Figure 2. FTIR spectra (a−c) and 2D maps (d−f) of PS-PnPMA obtained during heating at various pressures. (a,d) 0.001 bar; (b,e) 20 bar; and (c,f) 40 bar.

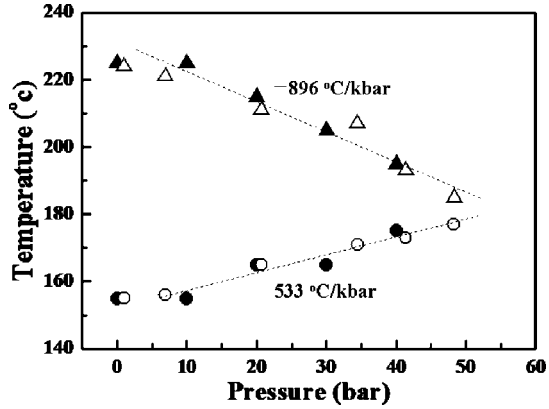

Figure 3. Changes in the LDOT (circle) and UODT (triangle) for PS-PnPMA with hydrostatic pressure measured by FTIR spectroscopy (filled symbols) and birefringence (open symbols).

To achieve this objective, in this study we investigated the transition temperatures of PS-PnPMA using pressure-dependent FTIR spectroscopy at various temperatures. Although commercially available diamond anvil cells (DACs) have been widely used to obtain pressure-dependent FTIR spectra for proteins,[31,32] they are limited to high pressures (>1 kbar) and poorer resolution (>100 bar). This means that DACs are not suitable for studying the pressure-dependent transitions of PS-PnPMA. This is because PS-PnPMA becomes completely disordered at pressures $P > \sim 80$ bar, and thus FTIR measurements of the pressure-dependent phase transitions require much better pressure control (∼1 bar).

We therefore designed a temperature-controlled pressure cell equipped with ZnSe windows capable of attaining a maximum pressure of ∼100 bar with a resolution of ∼1 bar, and temperatures up to ∼300 °C (see Experimental Section for details). Temperature-dependent FTIR spectra at constant P and pressure-dependent spectra at constant temperature were obtained from this pressure cell and analyzed by using two-dimensional correlation spectroscopy (2DCOS)[33,34] techniques. We found that at lower temperatures and as P increases, the PS main chains move ahead of PnPMA main chains. The mobility of the PnPMA chains is prohibited by the cluster formation of the alkyl side chains. On the other hand, at higher temperatures

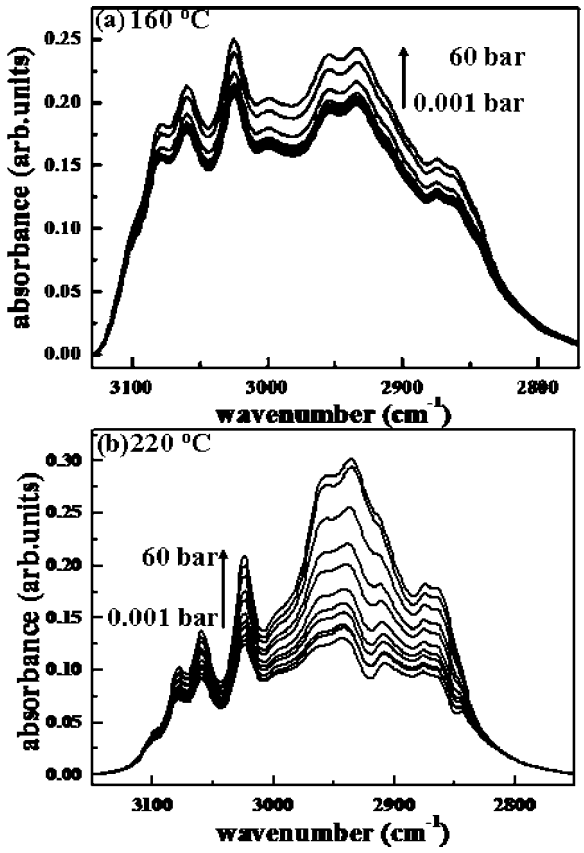

Figure 4. FTIR spectra of PS-PnPMA obtained during pressurization at two different temperatures: (a) 160 °C and (b) 220 °C.

the PnPMA block chains are more mobile than the PS block chains due to larger specific volume.

2. Experimental Section

PS-PnPMA was synthesized by the sequential, anionic polymerization of styrene and *n*-pentyl methacrylate in tetrahydrofuran at −78 °C under purified argon with *sec*-BuLi as an initiator. The weight-average molecular weight of PS-PnPMA was 48 860 g mol^{-1} determined by size exclusion chromatography using a multiangle laser light-scattering detector. The volume fraction of the PS block was 0.5.

FTIR spectra were measured at a spectral resolution of 4 cm^{-1} with a Bruker 66v/s FTIR spectrometer equipped with a liquid nitrogen-cooled MCT detector. The pressure cell made of stainless steel 304 had two ZnSe windows (13 mm in diameter × 5 mm in thickness) having high IR transmittance, four heaters with a thermocouple, and two empty holes: a vertical hole where a piston with two O-rings was placed and a horizontal hole, as shown in Figure 1. Under this geometry (the horizontal beam path on a sample), the optical path can change compared with that (the vertical beam path on a sample) commonly used in FTIR spectroscopy. However, because the temperatures and pressures were controlled outside of the vacuum chamber, the optical path length did not change during the entire experiments even for the horizontal geometry.

The sample cell consisted of a PS-PnPMA film sandwiched between two ZnSe windows. A PS-PnPMA film was cast from a toluene (1 wt % in solid) solution onto one ZnSe window, and the solvent was completely removed under vacuum at room temperature for 1 day. The second ZnSe window was then placed on the PS-PnPMA film, and the film was annealed at 120 °C for 1 day. The hydrostatic pressure (P) was controlled with a pressure regulator for the nitrogen gas which directly presses a piston against the top ZnSe window. Two O-rings on the piston inhibited the contact between the nitrogen gas and the PS-PnPMA film. An IR beam with a size of 2.5 mm in diameter came through the horizontal empty hole and passed near the center of the ZnSe windows. Finally, the pressure cell was inserted in an IR vacuum chamber maintained at 0.001 bar or less. Using this pressure cell, we could easily control P within 1 bar, and the cell temperature in the range 100−300 °C was controlled within 0.5 °C.

The FTIR spectra were measured by coadding 256 scans from 100 to 260 °C at intervals of 10 °C after equilibration for 20 min at the measurement temperature. Baseline correction was performed for all FTIR spectra before calculation of the 2D correlation spectra. The method employed to calculate the synchronous and asynchronous 2D correlation spectra has been described previously.[28,29] We employed two different experimental protocols: (1) temperature-dependent FTIR spectra at a fixed P (0.001, 10, 20, 30, and 40 bar) to obtain the transition temperatures at various P and (2) pressure-dependent FTIR spectra at a fixed temperature (160 and 220 °C) to study the transition mechanism in two different temperature regions.

3. Results and Discussion

Figure 2a−c show the FTIR absorption spectra of PS-PnPMA measured during heating from 100 to 260 °C at constant pressures of 0.001, 20, and 40 bar, respectively. The transition temperatures at each pressure were deduced from sudden changes in the 2D map of dA/dT (where A is the absorbance) as a function of wavenumber and temperature (T). At $P = 0.001$ bar, the LDOT and UODT of PS-PnPMA are determined to be 155 and 225 °C, respectively, which are essentially the same as those measured by birefringence methods at $P = 1$ bar (see Figure 3). With increasing P, the LDOT increases and the UODT decreases. For example, LDOT and UODT at 20 and 40 bar are 165 and 215 °C and 175 and 195 °C, respectively.

Figure 3 shows the changes in T_{LDOT} and T_{UODT} as a function of P, as determined from the FTIR spectra (Figure 2), from which dT_{LDOT}/dP and dT_{UODT}/dP are determined to be 533 and −896 °C/kbar, respectively. Also, the changes of these two transitions with P measured by birefringence method (open symbols) are shown in Figure 3. Two independent methods give almost the same results. FTIR spectroscopy detects the changes in the dipole moment, and thus molecular scales of two block chains, whereas the birefringence is related to the mesoscopic scale (10∼ 50 nm) of the microdomains of the block copolymer. Thus, we have successfully measured for the first time the pressure dependence of the transition temperatures by using the FTIR absorbance spectra with the aid of the 2D map.

However, the pressure coefficients given in Figure 3 are in variance with those (725 and −725 °C/kbar) obtained by SANS and birefringence for dPS-PnPMA.[20] Although the difference can be explained by the deuteration effect, the larger absolute value for dT_{UODT}/dP than dT_{LDOT}/dP for PS-PnPMA is consistent with the prediction (dT_{LDOT}/dP = 752 and dT_{UODT}/dP = −1025 °C/kbar) based on a compressible random phase approximation (cRPA).[27] According to the cRPA, the change of the effective interaction parameter (χ_{eff}) with temperature becomes much smaller at higher temperatures compared with lower temperatures; thus a small decrease of χ_{eff} due to P becomes a large decrease in the UODT compared with the increase in the LDOT.[26]

On the basis of the results presented in Figure 3, we performed pressure-dependent FTIR experiments at two temperatures

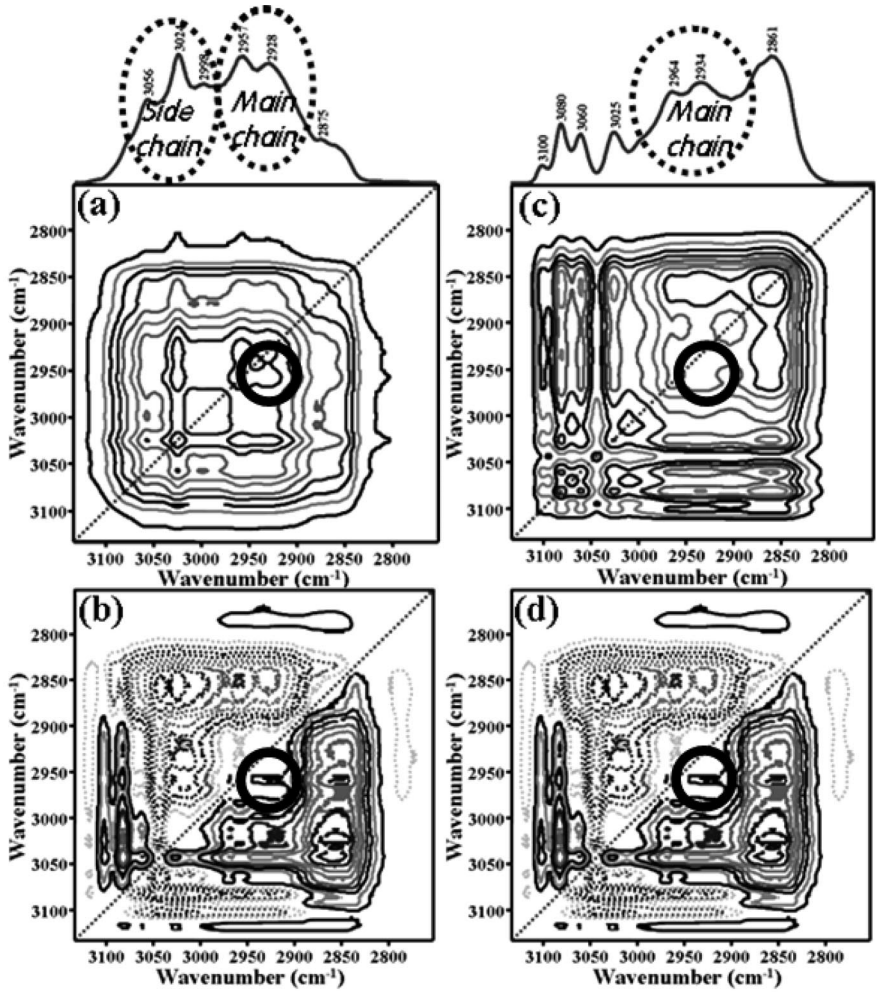

Figure 5. Synchronous (a,c) and asynchronous (b,d) 2D correlation analysis for PS-PnPMA at 160 °C. (a), and (b): low-pressure regime corresponding to the ordered state; (c),(d): high-pressure regime corresponding to the disordered state. Solid and dashed lines in the spectra represent positive and negative cross-peaks, respectively.

(160 and 220 °C), and the results are shown in Figure 4a,b. At 0.001 bar, these temperatures are within the temperature range of the ordered phase and are near the transitions, at 5 °C above the LDOT and 5 °C below the UODT, respectively. FTIR absorption spectra as a function of pressure at these two temperatures are shown in Figure 4. The pressure was changed from 0.001 to 60 at 5 bar intervals. Here, prominent IR bands were observed at 2928, 2957, 3024, and 3056 cm^{-1} and are assigned to the CH_2 asymmetric mode in the PS block, the CH_3 asymmetric mode in the PnPMA block, the ester methyl band in the PnPMA block, and the CH stretching mode in the PS ring, respectively.

Figure 5 shows the synchronous and asynchronous 2D correlation spectra obtained from the pressure-dependent FTIR spectra measured at 160 °C for the low- and high-pressure regimes. As noted in Figure 3, the low-pressure regime ($0.001 < P < 15$ bar) corresponds to the ordered state, and the high-pressure regime ($15 < P < 60$ bar) corresponds to the disordered state. The intensity of 2D correlation spectrum $X(\nu_1, \nu_2)$ is expressed by the dynamic spectrum of a system ($\tilde{y}(\nu,t)$) as follows:[33,34]

$$X(\nu_1, \nu_2) = <\tilde{y}(\nu_1, t)\tilde{y}(\nu_2, t')> \quad (1)$$

$$\tilde{y}(\nu, t) = y(\nu, t) - \bar{y}(\nu) \quad (2)$$

Here $y(\nu,t)$ is the perturbation-induced variation of a spectral intensity measured at a spectral variable along the external perturbation t (e.g., pressure in this study) between P_{max} (60 bar) and P_{min} (0.001 bar) and $\bar{y}(\nu)$ is the reference spectrum chosen as the spectrum [$\bar{y}(\nu,t)$] measured at the highest pressure (60 bar) employed in the FTIR experiment. In order to simplify the mathematical manipulation, $X(\nu_1, \nu_2)$ is treated as a complex number function that consists of two orthogonal (i.e., real and imaginary) components, known as the synchronous (Φ) and asynchronous (Ψ) 2D correlation intensities, respectively[33,34]

$$X(\nu_1, \nu_2) = \Phi(\nu_1, \nu_2) + i\Psi(\nu_1, \nu_2) = \frac{1}{\pi(P_{max} - P_{min})} \int_0^\infty \tilde{Y}(\nu_1, \omega) \cdot \tilde{Y}^*(\nu_2, \omega) d\omega \quad (3)$$

in which $\tilde{Y}$ and $\tilde{Y}^*$ are the Fourier transform and the conjugate of the Fourier transform of $\tilde{y}(\nu,t)$, respectively. The intensity of the peaks located at the diagonal positions in the synchronous 2D spectrum represents the overall susceptibility of the corresponding spectral region to change in spectral intensity as an external perturbation is applied to the system. Cross peaks located at the off-diagonal positions of the synchronous 2D spectrum represent simultaneous or coincidental changes of spectral intensities observed at two different spectral variables (ν_1 and ν_2). The sign of an asynchronous cross-peak provides information on the sequential order of events related to an

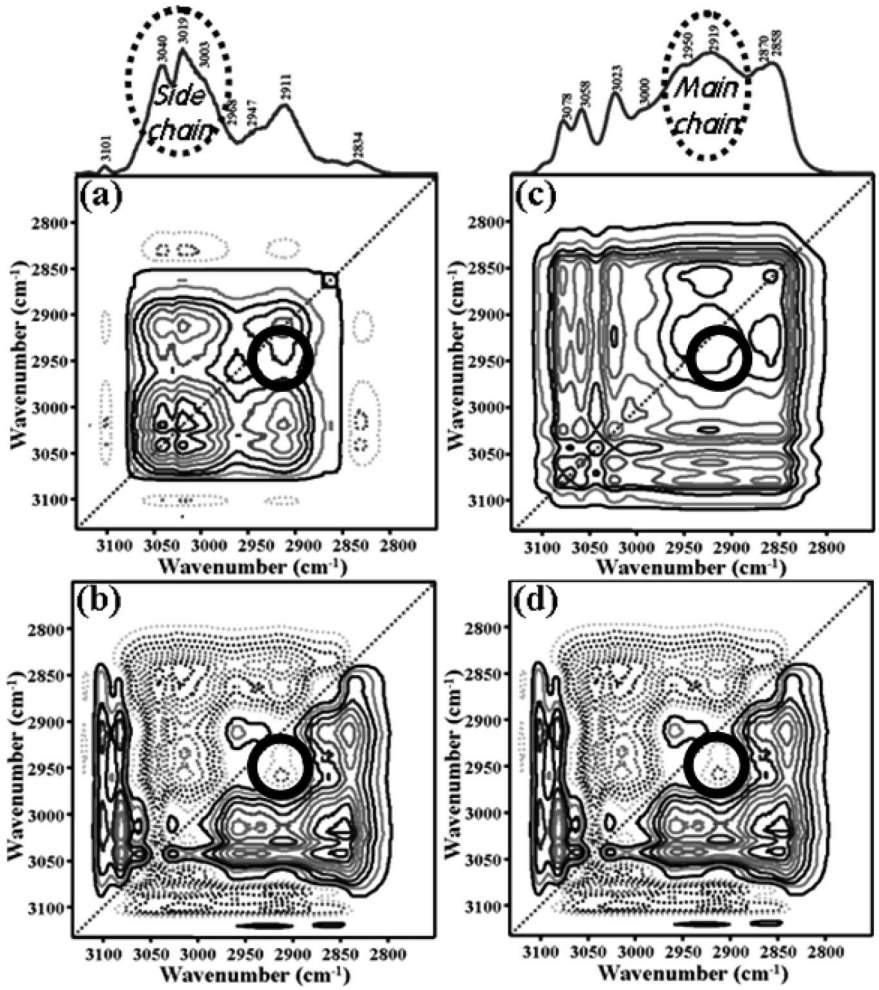

Figure 6. Synchronous (a,c) and asynchronous (b,d) 2D correlation analysis for PS-PnPMA at 220 °C. (a,b) Low-pressure regime corresponding to the ordered state. (c,d) High-pressure regime corresponding to the disordered state. Solid and dashed lines in the spectra represent positive and negative cross-peaks, respectively.

external variable. The sign of an asynchronous cross-peak is positive if the intensity change at ν_1 occurs at a time generally preceding that at ν_2. The sign becomes negative if the change at ν_1 occurs predominantly after ν_2. This sign rule is reversed if the synchronous correlation intensity at the same coordinate becomes negative. The set of sequential order rules described above is reasonably reliable provided that variation patterns of the spectral intensities during the observation period are largely monotonic.

It is seen in synchronous 2D correlation spectrum (Figure 5a) that the autopeaks assigned to both main chain groups and side chain groups become very strong, indicating that the degree of the main chain movement of both blocks is comparable to that of the side chain movement at lower pressure regime (in the ordered state). Also, the cross peak ($\nu_1 = 2928$ cm^{-1}, $\nu_2 = 2957$ cm^{-1}) marked by the solid circle is positive in both synchronous (Figure 5a) and asynchronous 2D correlation spectrum (Figure 5b). Since a band at 2928 cm^{-1} is assigned to the main chain of the PS block and another band at 2957 cm^{-1} is assigned to the main chain of the PnPMA block, the main chain of the PS block moves ahead the main chain of the PMMA block in the ordered state. This is because the motion of the PnPMA chains in the low-temperature ordered state is hindered by the nanosized cluster formation of the alkyl side chains.[29] In addition, the wide-angle X-ray scattering (WAXS) intensity corresponding to the cluster intensity becomes smaller with increasing temperature,[29] suggesting that the motion of the PnPMA block is more restricted at lower temperature.

With increasing pressure, the block copolymer becomes disordered. The autopeaks assigned to the main chain of both blocks are stronger than those assigned to the side chains of both blocks (see Figure 5c). This indicates that the degree of the main chain movement of both PS and PnPMA blocks at higher pressure regime (in the disordered state) is greater than that of the side chain movement reflecting high chain mobility. Also, due to the positive values of the cross peak ($\nu_1 = 2928$ cm^{-1}, $\nu_2 = 2957$ cm^{-1}) in both synchronous and asynchronous 2D correlation spectrum (Figure 5c,d), the main chain of the PS block moves prior to that of the PnPMA block. Thus, the moving sequence does not change upon transition from the ordered to the disordered phase. This finding suggests that pressure itself does not change much the degree of the cluster formation of PS-PnPMA at lower temperatures.

Figure 6 shows 2D correlation spectra obtained from the pressure dependent FTIR spectra at 220 °C for the low- and high-pressure regimes, corresponding to the ordered and disordered phases, respectively. It is seen in synchronous 2D correlation spectrum (Figure 6a) that the autopeaks assigned to the side chain of both blocks are stronger than those assigned to the main chains of both blocks. This indicates that the degree of the side chain movement of both blocks is greater than that of the main chain movement at lower pressure regime (in

the ordered state). Such behavior is distinctly different from results obtained for the lower-temperature ordered state (Figure 5a). At higher temperatures, the side chains become mobile even in the ordered state, whereas the main chain motion remains restricted due to the microdomain structure. Thus, cluster formation is not important at higher temperatures, which is consistent with results observed from the WAXS result (see Figure 3a in ref 29).

The cross peak ($\nu_1 = 2928$ cm^{-1}, $\nu_2 = 2957$ cm^{-1}) is negative in asynchronous 2D Correlation Spectrum (marked by the solid circle in Figure 6b), which is completely opposite the behavior at 160 °C. On the other hand, this cross peak is positive in synchronous 2D correlation spectrum (Figure 6a). Therefore, the main chains of the PnPMA block move prior to the PS chains at lower pressure. This can be attributed to the higher mobility of PnPMA. It is known that the thermal expansion coefficients of PnPMA and PS above 100 °C are 7.7×10^{-4} and 5.6×10^{-4} (1/K), respectively.[25]

In the disordered state (at higher P), because of a negative value of the cross peak ($\nu_1 = 2928$ cm^{-1}, $\nu_2 = 2957$ cm^{-1}) in asynchronous 2D correlation spectrum (Figure 6d) but a positive value of that peak in synchronous 2D correlation spectrum (Figure 6c), the main chains of the PnPMA block move prior to the PS chains. Namely, the moving sequence of main chains is the same as that in the ordered state (at lower *P*), indicating that the mobility of PnPMA is higher than PS even at higher pressure, despite the decrease in the mobility of both PnPMA and PS at higher pressures compared with that at lower pressures. From the above results, we consider that regardless of *P*, the cluster formation (or favorable interaction) is a major factor determining the phase behavior of PS-PnPMA at lower temperature, whereas the volume (or free volume) becomes more important at higher temperatures.

4. Conclusion

We investigated the effect of hydrostatic pressure on the phase transitions in PS-PnPMA by pressure-dependent FTIR spectroscopy and 2D correlation spectroscopy. The size of the LDOT−UODT closed-loop decreased with increasing pressure, consistent with results obtained from birefringence. At lower temperatures and with increasing pressure, the PS main chains move first relative to the PnPMA main chains, due to the restriction of the PnPMA chain mobility, arising from cluster formation of the alkyl side chains. At higher temperatures, the PnPMA block chains are more mobile than the PS block chains due to their larger specific volume. We conclude that for all pressures studied, the cluster formation (or directional interaction) is a dominant factor in the phase behavior of PS-PnPMA at low temperature, and the volume (or free volume) becomes more important at high temperatures. Furthermore, the cluster formation is relatively insensitive to pressure change, yet the free volume is strongly sensitive to *P*.

Acknowledgment. This work was supported by the National Creative Research Initiative Program supported by KOSEF and the Second Stage of Brain Korea 21 Project.

Note Added after ASAP Publication. This paper was published ASAP on November 1, 2008. Text was updated in the abstract and Figure 2 caption. The revised paper was reposted on November 6, 2008.

References and Notes

(1) Hashimoto, T. In *Thermoplastic Elastomers*; Legge, N. R.; Holden, G.; Schroeder, H. E.; Eds.; Hanser: New York, 1987.

(2) Hamley, I. W. *The Physics of Block Copolymers*; Oxford University Press: New York, 1998.

(3) *Developments in Block Copolymer Science and Technology*; Hamley, I. W., Ed.; John Wiley & Sons Ltd.: Chichester, England, 2004.

(4) Kim, J. K.; Lee, J. I.; Lee, D. H. *Macromol. Res.* **2008**, *16*, 267.

(5) Fredrickson, G. H.; Bates, F. S. *Annu. Rev. Mater. Sci.* **1996**, *26*, 501.

(6) Helfand, E.; Wasserman, Z. R. In *Developments in Block Copolymers*; Goodman, I., Ed., Applied Science: New York, 1982.

(7) Leibler, L. *Macromolecules* **1980**, *13*, 1602.

(8) Bates, F. S.; Fredrickson, G. H. *Annu. Rev. Phys. Chem.* **1990**, *41*, 525.

(9) Bates, F. S. *Science* **1991**, *251*, 898.

(10) (a) Han, C. D.; Kim, J.; Kim, J. K. *Macromolecules* **1989**, *22*, 383. (b) Han, C. D.; Baek, D. M.; Kim, J. K. *Macromolecules* **1990**, *23*, 561. (c) Han, C. D.; Baek, D. M.; Kim, J. K.; Ogawa, T.; Sakamoto, N.; Hashimoto, T. *Macromolecules* **1995**, *28*, 5043.

(11) Russell, T. P.; Karis, T. E.; Gallot, Y.; Mayes, A. M. *Nature* **1994**, *368*, 729.

(12) Hashimoto, T.; Hasegawa, H.; Katayama, H.; Kamigaito, M.; Sawamoto, M.; Imai, M. *Macromolecules* **1997**, *30*, 6819.

(13) Pollard, M.; Russell, T. P.; Ruzette, A. V. G.; Mayes, A. M.; Gallot, Y. *Macromolecules* **1998**, *31*, 6493.

(14) Ruzette, A. V. G.; Banerjee, P.; Mayes, A. M.; Pollard, M.; Russell, T. P.; Jerome, R.; Slawecki, T.; Hjelm, R.; Thiyagarajan, P. *Macromolecules* **1998**, *31*, 8509.

(15) Weidisch, R.; Stamm, M.; Schubert, D. W.; Arnold, M.; Budde, H.; Horing, S. *Macromolecules* **1999**, *32*, 3405.

(16) Hasegawa, H.; Sakamoto, N.; Takeno, H.; Jinnai, H.; Hashimoto, T.; Schwahn, D.; Frielinghaus, H.; Janben, S.; Imai, M.; Mortensen, K. *J. Phys. Chem. Solids* **1999**, *60*, 1307.

(17) Ryu, D. Y.; Shin, C.; Cho, J.; Lee, D. H.; Kim, J. K.; Lavery, K. A.; Russell, T. P. *Macromolecules* **2007**, *40*, 7644.

(18) Ryu, D. Y.; Jeong, U.; Kim, J. K.; Russell, T. P. *Nat. Mater.* **2002**, *1*, 114.

(19) Ryu, D. Y.; Jeong, U.; Lee, D. H.; Kim, J.; Youn, H. S.; Kim, J. K. *Macromolecules* **2003**, *36*, 2894.

(20) Ryu, D. Y.; Lee, D. J.; Kim, J. K.; Lavery, K. A.; Russell, T. P.; Han, Y. S.; Seung, B. S.; Lee, C. H.; Thiyagarajan, P. *Phys. Rev. Lett.* **2003**, *90*, 235501.

(21) Ryu, D. Y.; Lee, D. H.; Jeong, U.; Yun, S. H.; Park, S.; Kwon, K.; Sohn, B. H.; Chang, T.; Kim, J. K. *Macromolecules* **2004**, *37*, 3717.

(22) Ryu, D. Y.; Lee, D. H.; Jang, J.; Kim, J. K.; Lavery, K. A.; Russell, T. P. *Macromolecules* **2004**, *37*, 5851.

(23) Li, C.; Lee, D. H.; Kim, J. K.; Ryu, D. Y.; Russell, T. P. *Macromolecules* **2006**, *39*, 5926.

(24) Lavery, K. A.; Sievert, J. D.; Watkins, J. J.; Russell, T. P.; Ryu, D. Y.; Kim, J. K. *Macromolecules* **2006**, *39*, 6580.

(25) Li, C.; Li, G. H.; Lee, D. H.; Kim, J. K. *Polymer* **2007**, *48*, 4235.

(26) (a) Li, C.; Li, G. H.; Moon, H. C.; Lee, D. H.; Kim, J. K.; Cho, J. *Macromol. Res.* **2007**, *15*, 656. (b) Moon, H. C.; Han, S. H.; Kim, J. K.; Li, G. H.; Cho, J. *Macromolecules.* **2008**, *41*, 6793.

(27) (a) Cho, J. *Macromolecules* **2004**, *37*, 10101. (b) Cho, J.; Kwon, Y. K. *J. Polym. Sci., Polym. Phys. Ed* **2003**, *41*, 1889.

(28) Kim, H. J.; Kim, S. B.; Kim, J. K.; Jung, Y. M.; Ryu, D. Y.; Lavery, K. A.; Russell, T. P. *Macromolecules* **2006**, *39*, 408.

(29) Kim, H. J.; Kim, S. B.; Kim, J. K.; Jung, Y. M. *J. Phys. Chem. B* **2006**, *110*, 23123.

(30) Jung, Y. M.; Kim, H. J.; Ryu, D. Y.; Kim, S. B.; Kim, J. K. *J. Mol. Struct.* **2006**, *799*, 96.

(31) Dzwolak, W.; Kato, M.; Taniguchi, Y. *Biochim. Biophys. Acta* **2002**, *1595*, 131.

(32) Edwards, C. M.; Butler, I. S. *Coord. Chem. Rev.* **2000**, *199*, 1.

(33) (a) Noda, I. *Bull. Am. Phys. Soc.* **1986**, *31*, 520. (b) Noda, I. *J. Am. Chem. Soc.* **1989**, *111*, 8116. (c) Noda, I. *Appl. Spectrosc.* **1990**, *44*, 550. (d) Noda, I. *Appl. Spectrosc.* **1993**, *47*, 1329. (e) Noda, I. *Appl. Spectrosc.* **2000**, *54*, 994.

(34) Noda, I.; Ozaki, Y. *Two-Dimensional Correlation Spectroscopy: Applications in Vibrational Spectroscopy*; John Wiley & Sons, Inc.: New York, 2004.

JP806019N